APPLIED AND ENVIRONMENTAL MICROBIOLOGY, Nov. 2000, p. 5092–5098 Vol. 66, No. 11
0099-2240/00/$04.00+0

Heavy Metal Coprecipitation with Hydrozincite [$Zn_5(CO_3)_2(OH)_6$] from Mine Waters Caused by Photosynthetic Microorganisms

FRANCESCA PODDA,[1] PAOLA ZUDDAS,[1] ANDREA MINACCI,[2] MILVA PEPI,[2] AND FRANCO BALDI[2]*

Department of Earth Sciences, University of Cagliari, 09127 Cagliari,[1] and Department of Environmental Sciences, University Cà Foscari, 30122 Venice,[2] Italy

Received 24 April 2000/Accepted 21 July 2000

An iron-poor stream of nearly neutral pH polluted by mine tailings has been investigated for a natural phenomenon responsible for the polishing of heavy metals in mine wastewaters. A white mineralized mat, which was determined to be hydrozincite [$Zn_5(CO_3)_2(OH)_6$] by X-ray diffraction analysis, was observed in the stream sediments mainly in spring. The precipitate shows a total organic matter residue of 10% dry weight and contains high concentrations of Pb, Cd, Ni, Cu, and other metals. Scanning electron microscopy analysis suggests that hydrozincite is mainly of biological origin. Dormant photosynthetic microorganisms have been retrieved from 1-year-old dry hydrozincite. The autofluorescent microorganisms were imaged by a scanning confocal laser microscope. A photosynthetic filamentous bacterium, classified as *Scytonema* sp. strain ING-1, was found associated with microalga *Chlorella* sp. strain SA1. This microbial community is responsible for the natural polishing of heavy metals in the water stream by coprecipitation with hydrozincite.

Abandoned mines present a high environmental hazard in all countries today. In several parts of the world where mining activities have shut down, the problem of the control and reclamation of polluted areas for new activities arises. The polishing of metals from a mining area is a difficult task. The transformation of metals into harmless species or their removal in a suitable recycled mineral form such as carbonates (1, 15) is a possible solution for the remediation of a mining area. Therefore, research in this field continues, with the isolation of new strains with more-successful mechanisms for the reduction of metal toxicity.

At Ingurtosu (southwestern Sardinia, Italy) lead and zinc sulfide ore deposits were mined until 1968 and tailings were deposited along the Rio Naracauli creek. The Montevecchio-Ingurtosu deposit consists of galena-sphalerite veins in a quartz gangue containing iron, calcium, and magnesium carbonate minerals. Pyrite, chalcopyrite, barite, cerussite, and anglesite are the most commonly associated minerals (22). Previous studies in this area have shown that waters are highly polluted by heavy metals, in spite of their near-neutral pH (4–6, 30).

The aim of this work was to study the fate of leached toxic metals from sulfide ore tailings in the upper part of the Rio Naracauli creek, where natural polishing of metals in waters occurred as a result of a very large growth of photosynthetic microbial populations that colonized sediments in spring and deposited a white mat on the creek bed. The role of this photosynthetic community adapted to toxic metals and the mechanism of metal sequestration were studied.

Study area and samplings. The Rio Naracauli flows in a 30.2 km^2 basin west of the Ingurtosu mine in the Arburese mine district in southwestern Sardinia (Fig. 1). The river is about 8.2 km long and flows into the western Mediterranean Sea. The Rio Naracauli has a very limited flow, particularly in the upper part. Upstream it receives drainage from mine tailings on the left, and downstream it receives drainage from three adits: the Rio Pitzinurri (outlet A), the Ledoux mine gallery (outlet B), and the Rio Bau (outlet C). The hydrogeological details of this area have been reported by Pala et al. (21).

A total of 14 stations (stations 1 to 11 in the creek and stations A to C in the three tributaries) were chosen along 3.4 km of the Rio Naracauli (Fig. 1). Station 1 was located at the tailings pond. In stations 2 to 4, a photosynthetic microbial population visibly encrusted the sediments with a green mat in spring, which developed into white material, particularly at stations 3 and 4. This is an annual event that varies in intensity depending on the meteorological conditions. The white precipitate is then mechanically transported away by rainfalls. Stations 5 to 7 were located after the Rio Pitzinurri tributary (sample A). In the sediments of these stations white precipitate residues were still visible. Stations 8 to 10 were located after the Ledoux gallery (sample B). Station 11 was located downstream from the Rio Bau tributary (sample C), where white deposits were not observed.

Hydrozincite determination and distribution. The white mineralized material at stations 3 and 4 was collected for mineralogical, chemical, and microscopic analyses in April 1997, concomitantly with a photosynthetic microorganism bloom. At station 4 the precipitated material was very abundant. The mineralogical characterization of the mineral precipitate was performed by X-ray powder diffraction (XRD) with a diffractometer (Philips; model PW 1710) with CuKα radiation. The mineral was determined to be crystalline hydrozincite [$Zn_5(CO_3)_2(OH)_6$] (Fig. 2). Minor minerals, such as quartz and calcite, were also observed. XRD spectra also showed a significant background noise, which was due to the presence of organic matter. Samples of the white solid precipitate were also collected at other sites along the Rio Naracauli creek, and their XRD spectra showed a significant decrease in crystalline hydrozincite from sample 6 to sample 7 (Fig. 2). A white, soft, unconsolidated mud was also collected from stations 8 to 10. This precipitate was identified as amorphous material made up of Zn, Si, and oxygen (30). From sample 8 to the last station, hydrozincite was not detected.

The concentrations of the main selected chemical components in hydrozincite precipitates from station 4 are reported in Table 1. The organic carbon content was determined by the

* Corresponding author. Mailing address: Department of Environmental Sciences, University Cà Foscari, La Celestia, Via Castello 2737/b, I-30122 Venice, Italy. Phone: 39-041-2578432. Fax: 39-041-5281494. E-mail: baldi@unive.it or baldi@unisi.it.

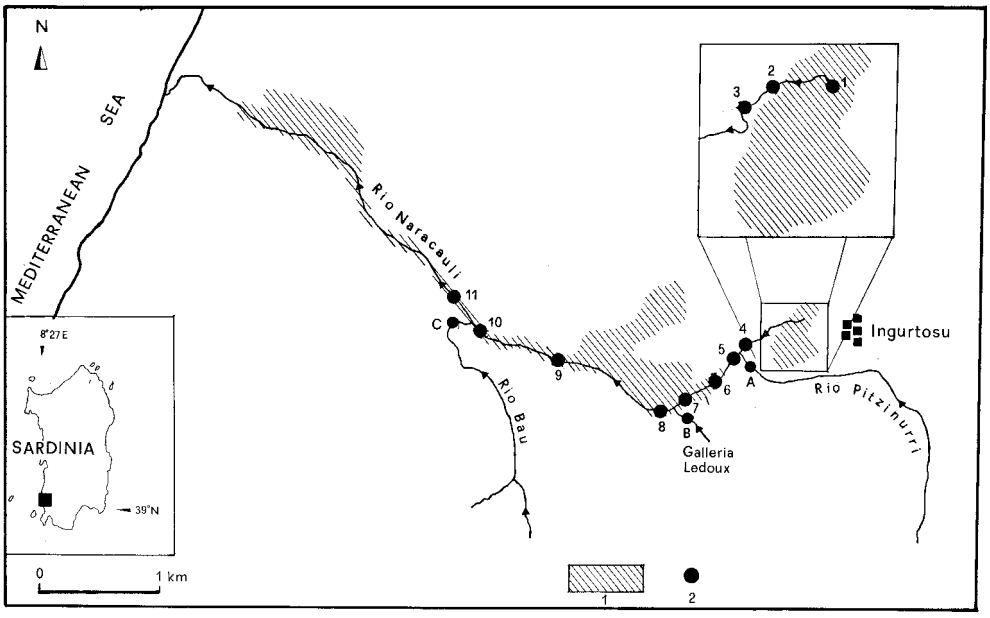

FIG. 1. Schematic map of the sampling area, with tailings distribution (hatched areas). Samples 1 to 11 (●) are from the Rio Naracauli stream; samples A to C were collected in the tributaries before the inflows.

oxidation method (3). A white solid sample (1.0 g) was finely ground and dried at 105°C. The sample was treated with a mixture of 20 ml of $K_2Cr_2O_7$ (0.17 M) and 20 ml of concentrated H_2SO_4 at room temperature. Excess potassium dichromate was titrated with ferrous sulfate according to the Walkley-Black method (28).

Elemental characterization of the white precipitate materials was performed with 0.25 g of the sample. A high-purity mixture of 5 ml of concentrated HCl and 7.5 ml of concentrated HNO_3 was added to the solid sample in a Teflon vessel. The sample was then heated by microwave (model CEM-MDS 2100) for 25 min. The sample was then cooled, 2 ml of H_2O_2 (30% by volume) was added, and the sample was once more microwaved for 17 min for final digestion. The final solution was filtered and made up to 25 ml using Milli Q water. All the elements were determined by inductively coupled plasma-atomic emission spectroscopy. As shown in Table 1 the Zn content in the analyzed sediment, considering the presence of contaminant phases, is in good agreement with the theoretical formulae of hydrozincite (17). Hydrozincite coprecipitates high concentrations of other toxic elements such as Pb, Cd, Cu, and Ni, in agreement with the decrease in metals observed in the stream waters. Coprecipitation of these metals occurred in concomitance with the formation of hydrozincite, by a mechanism similar to that previously reported for strontium precipitation in calcite mineral (12). The high Ca concentration was due to the presence of calcite and secondary $CaSO_4$ traces in hydrozincite. The total Fe concentration was very low, as observed in the depositing waters.

Microbiological evidence of hydrozincite formation. Further mineralogical analyses were performed on a Cambridge 250 MK3 scanning electron microscope (SEM) associated with an energy-dispersive X-ray system (EDX; LINK AN 10/55S). The biological origin of hydrozincite was clearly pointed out by

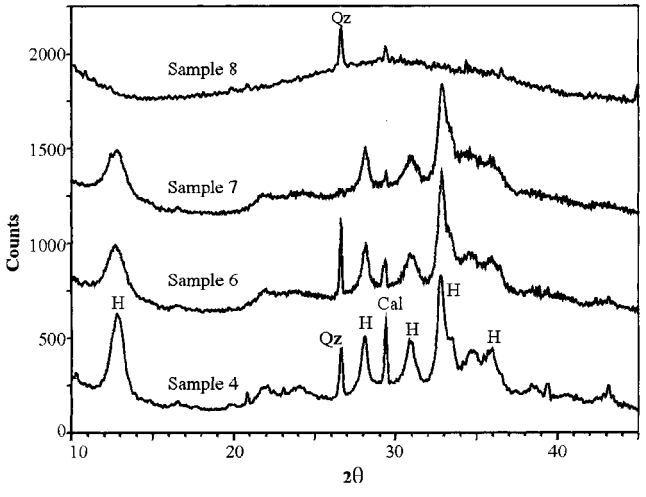

FIG. 2. XRD spectra of some selected precipitates in Rio Naracauli, with relative intensity peaks of hydrozincite (H), calcite (Cal), and quartz (Qz).

TABLE 1. Organic matter[a] metals, and sulfate concentrations in the hydrozincite sediment sampled at station 4 in Rio Naracauli

Element or compound	Concn (mg kg^{-1})
Zn	519,000
Pb	6,500
Cd	540
Fe	1,040
Mn	30
Cu	260
Ni	370
Co	4
Ca	10,300
Mg	530
K	540
SO_4^{2-}	6,600

[a] The concentration of organic matter was 10%.

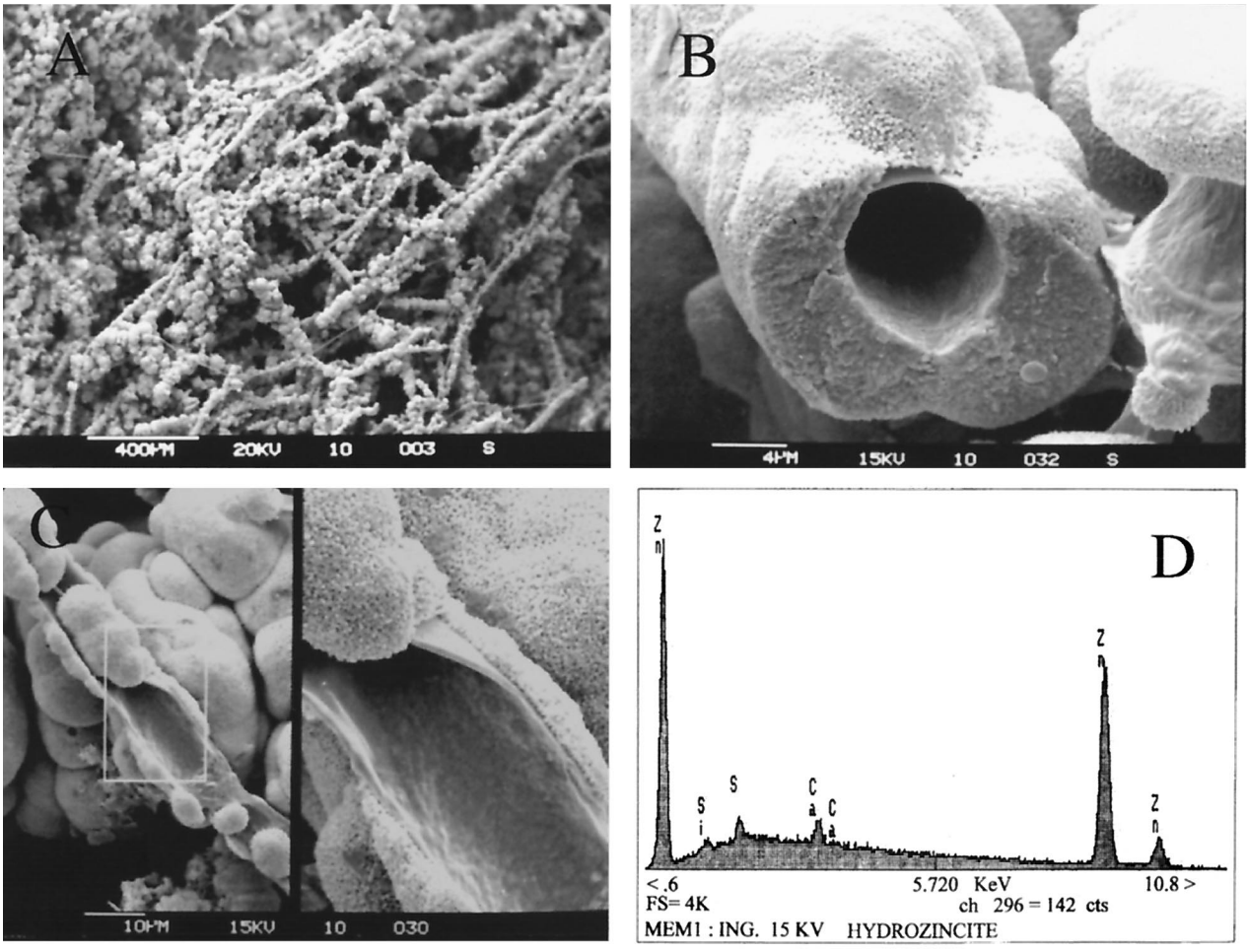

FIG. 3. Photos of white precipitate obtained by SEM. (A) Formation of tubing network of hydrozincite produced by microorganisms. Bar, 400 μm. (B) Detail of a tubing section giving a better view of the biological origin of hydrozincite. Bar, 4 μm. (C) (Left) Further details with naked parts of a sheath. Bar, 10 μm. (Right) Close-up detail of the sheath on a framed rectangle. (D) EDX elemental analysis of a sheath encrustation revealing high Zn concentrations.

SEM observations (Fig. 3). The precipitate of minerals around biological structures formed a network of microscopic tubing (Fig. 3A). In detail the mineral seems to encrust filamentous bacteria (Fig. 3B). Broken filaments showed an open internal diameter of 6.0 ± 0.8 μm. At a greater magnification, SEM analysis showed a small amount of "naked" sheath under the inorganic encrustation (Fig. 3C, left). In more detail, spherical and rough particles of different sizes strongly adhered to the bacterial sheath (Fig. 3C, right). Hydrozincite microspherical particles are approximately 0.2 μm in diameter. Spherical particles are cemented together in long tubing and produce a very hard crust, coating the pebbles of the bottom sediments. EDX element analysis of the precipitate confirmed the presence of Zn, with minor Si, Ca, and S in the mineral phase (Fig. 3D).

To further demonstrate the biological origin of hydrozincite in Rio Naracauli, about 2.0 g of the 1-year-old solid sample, stored in dark, dry conditions and sterile vials, was incubated in a flask under dim light at room temperature, by adding a 1:10-diluted, conventional BG-11 medium (American Type Culture Collection medium 616) for cyanobacterial isolation. After a few days of incubation, filaments formed from the white precipitate (Fig. 4A) and were coated by green filaments (Fig. 4B).

The autofluorescence of the microbial community due to photosynthetic pigments was observed by confocal microscopy. The white solid specimen was soaked in sterile buffered water and then observed without any treatment under light transmission and in fluorescence modes with scanning confocal laser microscopy (SCLM) (Bio-Rad Microscience Division; model MRC-500); the microscope was equipped with a krypton-argon laser, with maximum emission at 488 nm. The cells emit red autofluorescence due to the photosynthetic pigments contained in them. Three-dimensional images were taken with the procedure reported by Baldi et al. (2). Images were collected in the transmission mode (Fig. 4C and F) and in the fluorescence mode (Fig. 4D and G). A terminal heterocyst due to the lack of photosynthetic apparatus (Fig. 4D) was present, as confirmed by the presence of a thick-wall cell observed under the light transmission mode (Fig. 4C). From these two photographs it was evident that a new filament of cyanobacterium was produced inside the tubing cavity, which was formed by hydrozincite precipitation around the microbial sheath.

The cyanobacterium was identified as *Scytonema* sp. strain ING-1 based on its morphological characteristics. It forms uniseriated and sheathed trichomes with false branches made up of hormogonia and a single terminal heterocyst. It colonizes mainly freshwater benthic habitats (7). In flask cultures, *Scytonema* sp. strain ING-1 produced gel-holding masses of trichomes strongly adhering to glass surfaces and/or sediment gravels of the Rio Naracauli creek.

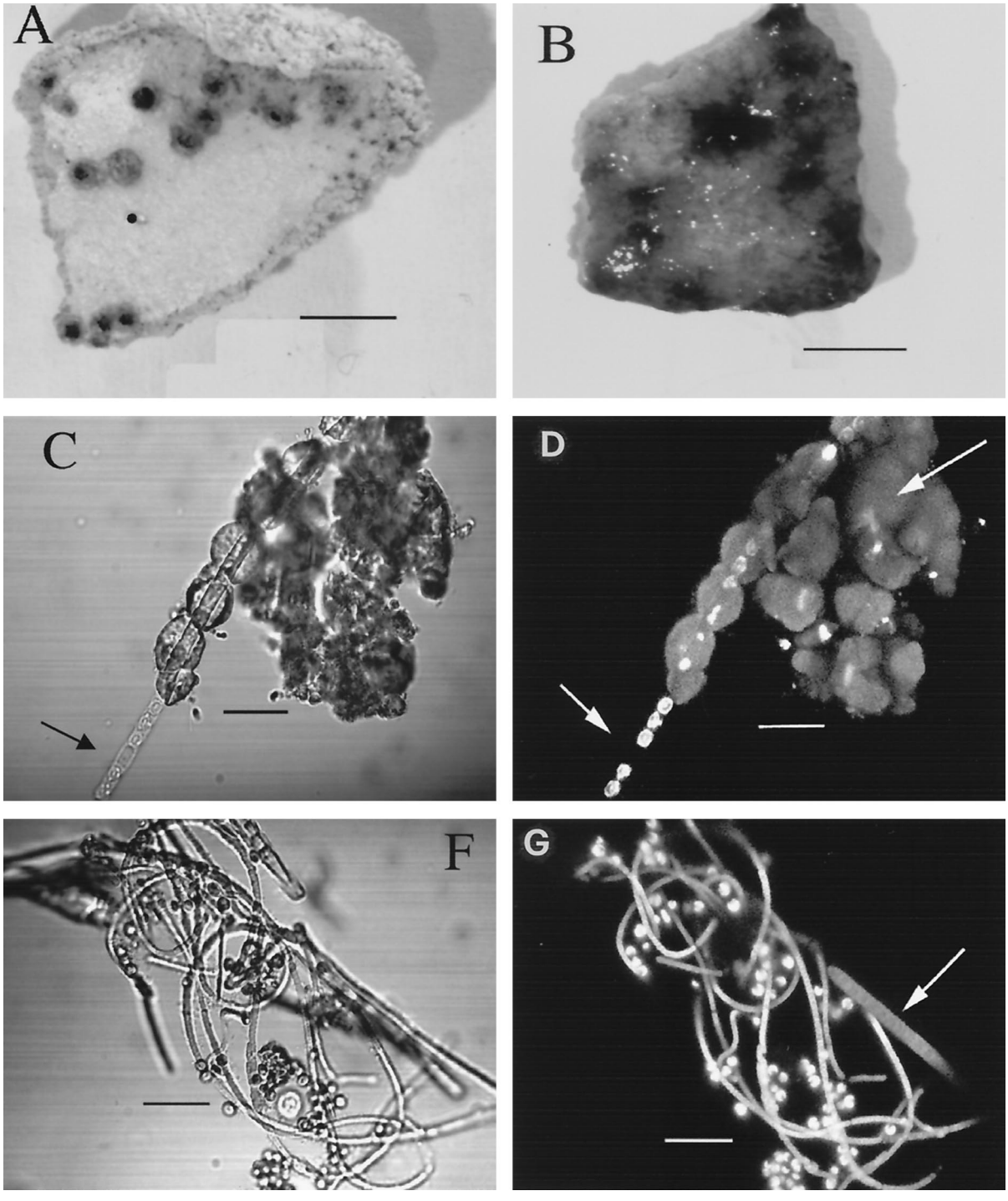

FIG. 4. (A) Photograph of a piece of old, dried, consolidated hydrozincite with dark spots, with cyanobacterium *Scytonema* sp. in a dormant state. Bar, 0.5 cm. (B) The same piece of hydrozincite after a period of incubation in BG-11 medium (diluted 1:10) under dim light, clearly showing growth of *Scytonema* sp., which was entrapped in the hydrozincite matrix and which forms blue-green filaments. Bar, 0.5 cm. (C) In the transmission mode the *Scytonema* sp. clearly grows out of the hydrozincite tubing. A thick-wall heterocyst (short arrow) is clearly visible. Bar, 12, μm. (D) The same image by SCLM shows single autofluorescent cells of a *Scytonema* sp. Autofluorescence is due to chlorophyll *a* encapsulated in the sheath. Where the heterocyst occurs (short arrow), no autofluorescence appears, since the photosynthetic apparatus is degenerated. Moreover, hydrozincite emits fluorescence (long arrow). Bar, 12 μm. (F) Coculture of *Scytonema* sp. and the microalga *Chlorella* sp. The cyanobacterium shows filaments of different diameters. Bar, 12 μm. (G) The same image taken by SCLM (the sheath of the *Scytonema* sp. becomes empty and wide with aging and autofluorescence [arrow]). Bar, 12 μm.

After 7 days of incubation another photosynthetic coccoid microorganism, with a diameter of 4.0 to 4.5 μm was observed (Fig. 4F and G). The microalga was classified as *Chlorella* sp. strain SA-1 by the size and spherical shape of a nonmotile cell with a peripheral chloroplast. The microalga remained as a single cell, well anchored to the cyanobacterium sheath network, until both microorganisms were isolated under laboratory conditions.

TABLE 2. Analytical data for the water sampled in the Rio Naracauli and tributaries

Sample	Distance (m)	Temp (°C)	pH	E_h (mV)	Cond.[a] (μS cm^{-1})	TDS (mg liter^{-1})	Concn of indicated element or compound												
							Major (mg liter^{-1})								Trace (μg liter^{-1})				
							Na	K	Mg	Ca	Zn	Cl	SO_4^{2-}	HCO_3^-	Cd	Pb	Cu	Ni	Co
1	0	17	6.4	491	1,602	1,429	53	6.4	25	91	348	84	794	29	3,280	1,060	31	170	6
2	200	17	6.4	516	1,435	1,189	55	7.5	29	99	218	93	662	27	2,150	695	14	123	7
3	300	17	7.1	451	2,020	1,536	71	8.6	93	246	58	110	834	215	495	270	15	180	3
4	620	20	7.7	449	1,910	1,495	72	8.8	93	244	29	110	860	139	420	60	5	140	2
A	621	16	6.6	379	570	320	59	3.0	13	33	2	96	39	109	17	4	n.d.[b]	4	n.d.
5	630	16	7.2	435	1,240	836	71	5.9	46	119	24	110	368	152	245	88	5	41	1
6	900	18	7.6	454	1,743	1,321	78	8.0	75	193	28	123	725	154	410	160	7	61	1
7	1,300	17	7.8	451	1,734	1,291	79	7.8	76	191	15	121	716	147	360	71	4	48	1
B	1,350	18	8.3	428	878	486	60	3.8	31	67	2	95	159	139	15	190	15	42	7
8	1,600	18	8.3	413	897	578	67	4.1	32	76	2	88	191	190	45	18	2	13	1

[a] Cond., conductivity.
[b] n.d., not determined.

Pigment analysis was carried out on the following three microorganisms: *Scytonema* sp. strain ING-1, *Chlorella* sp. strain SA-1 grown in a liquid BG-11 medium, and the reference strain *Chlamydomonas reinhardtii*, grown in R medium (19). Each culture was filtered through nitrocellulose filters (0.2-μm pore size; Sartorius). Cells were harvested, and pigments were extracted by a 3-ml acetone-methanol (7:2) solution. Absorption spectra of pigments were recorded with a spectrophotometer from 300 to 800 nm (Shimadzu; UV-360). In the cyanobacterium, pigment spectra showed peaks of phycocyanin and phycoerythrocyanin at 617 and 582 nm, respectively, plus a peak of chlorophyll *a* at 663 nm. Large amounts of carotenoids were also produced, as confirmed by absorption peaks at 432 and 478 nm.

In the coccoid *Chlorella* sp. the pigment emits at 662 nm corresponding to chlorophyll *a*, and a large peak at 439 nm, due to carotenoids, was also determined. This pigment spectrum was similar to that of *C. reinhardtii*, confirming that the coccoid photosynthetic cell was a microalga.

The Alcian blue stain technique (20) was used to determine the presence of acidic polysaccharide produced by the cultivated photosynthetic community isolated from the white precipitates in a BG-11 medium, while carbofuchsin was used for counterstaining. The specimen was heat fixed on a glass slide, and the blue-stained specimen was observed under a light transmission microscope. Under the fluorescence mode, the precipitate mineral coating the sheath was also autofluorescent (Fig. 4D), as shown by the emission of a strong green light. This observation suggested the presence of a molecular secretion by the microorganism involved in the formation of hydrozincite. In fact after several weeks of incubation of the *Scytonema* sp., older sheaths became progressively empty and wide and emitted a similar green autofluorescence (Fig. 4G). The polysaccharide sheath also became acidic, as confirmed by staining with Alcian blue. Hormogonia and young narrow filaments were not stained by Alcian blue. In the formation of hydrozincite, the role of *Chlorella* sp. is probably that of reinforcing the filament structures and sequestering even more cations, because of its own acidic polysaccharide capsule, which is also positive to Alcian blue staining.

Water analysis. During the same sampling campaign, 14 superficial water samples from the Rio Naracauli were collected at the 11 stations plus the three outflows (A, B, and C). The water samples were filtered through 0.45-μm-pore-size polycarbonate filters by a metal-free filtering apparatus (Nucleopore). Filtered water samples were collected into previously acid-cleaned polyethylene bottles. For metal analysis, water subsamples were acidified by HNO_3 (Aristar grade; Merck) to reach a final 1% concentration. For anion analyses, nonacidified water subsamples were stored in the dark at 4°C.

Parameters such as the temperature (degrees Celsius), conductivity (microsiemens per centimeter), pH, redox potential (millivolts), and alkalinity of the waters were measured in situ (14). The major cations, Ca^{2+}, Mg^{2+}, Na^+, K^+, Zn^{2+}, and Cd^{2+}, were determined by inductively coupled plasma-atomic emission spectroscopy (ARL3520). Other trace elements, Pb^{2+}, Cu^{2+}, Ni^{2+}, and Co^{2+}, were determined by inductively coupled plasma-mass spectroscopy (Perkin-Elmer; ELAN 5000). These analytical procedures and their reproducibilities and sensitivities have been reported by Cidu (8).

In filtered nonacidified subsamples, the major anions (CI^- and SO_4^{-2}) were analyzed by high-pressure liquid chromatography on an instrument (Dionex) equipped with an AS12A-Sc column, a conductivity detector (model CDM1), and a carbonate-bicarbonate mobile phase (2.7 and 0.3 mM) at 1.5 ml min^{-1} (16). Analytical data for the waters from stations 1 to 8, sampled in the area affected by hydrozincite deposition, are reported in Table 2.

Based on the major components, the waters show a dominant $CaSO_4$-$MgSO_4$ chemical composition, except for sample A, which represents the Rio Pitzinurri tributary. At stations 1 and 2 the main cation in the water was Zn^{2+}; in the other stations the main cations were Ca^{2+} and Mg^{2+}.

Along the analyzed stream section, the salinity as total dissolved solids (TDS) shows large variations. Between stations 1 and 2, the TDS decrease was due to the dilution effect of sulfate and metal-poorer waters. Conversely, TDS increased between stations 2 and 3 due to a significant input of HCO_3^--rich waters from tailings located along the stream (Fig. 1). A rapid increase in the pH took place from station 2 to stations 3 and 4 due to photosynthetic activity. This process was associated with a decrease in HCO_3^-, especially between stations 3 and 4, where hydrozincite precipitation occurred. Toxic metals Zn^{2+}, Cd^{2+}, Pb^{2+}, Ni^{2+}, and Cu^{2+} decreased dramatically in waters at stations 3 and 4, concurrent with carbonate formation, and more gradually at the other stations. From the first station to the fourth Zn, Cd, Pb, and Cu contents in waters decreased by 92, 87, 94, and 84% respectively.

Chemical speciation, partial CO_2 pressure (pCO_2), and equilibrium calculations for water samples were performed by the WATEQP computer program (C. A. J. Appelo, WATEQP—a computer program for equilibrium calculations of water analysis, Institute of Earth Sciences, Free University of Amsterdam, 1988). The saturation index (SI) with respect to

the mineral phases was calculated as log (IAP/K_s), where IAP is the ionic activity product and K_s is the equilibrium constant at the water temperature. The SI in the waters was also calculated for the following carbonates: hydrozincite, calcite, smithsonite ($ZnCO_3$), and cerussite ($PbCO_3$). Hydrozincite saturation equilibrium was reached at station 3 ($SI_H = -0.04$), and it was due to a significant input of HCO_3^--rich waters from other tailings between stations 2 and 3 along the Rio Naracauli. The further oversaturation equilibrium conditions ($SI_H = 1.50$) reached in station 4 are not due to chemical inputs or outputs but to the photosynthetic activities of identified microorganisms. In the waters of stations 3 and 4, chemical variations were observed only for HCO_3^-, Zn^{2+}, Pb^{2+}, and Cd^{2+}, while other ions did not change. The SI with respect to hydrozincite formation was also achieved in stations 6 and 7. Calcite equilibrium was reached at station 3, and conditions stayed close to equilibrium up to the last sampling site. The waters were undersaturated with respect to smithsonite and cerussite at all stations.

Conclusions. The involvement of cyanobacteria in the formation of calcium carbonate (11–13, 27) and other types of carbonates (18, 23) is well documented. This precipitation is helped by photosynthesis metabolism, which in the aqueous system shifts the inorganic C species equilibrium to carbonates (25). The biomineralization of zinc carbonates has not been reported, except by Kalin (18), who did not specify the mineralogical phase of the zinc carbonate.

Cell envelope characteristics are crucial for mineral nucleation (13). Since in natural conditions microbial organisms have electronegative surfaces (9), they easily bind metals to their envelopes. In our study several observations support the epicellular biomineralization of hydrozincite on cyanobacterial sheaths induced by alkalization in the microenvironment due to CO_2 fixation from dissolved HCO_3^- and release of OH^- during photosynthesis. In fact, an increase (rapid) in pH associated with a decrease in HCO_3^- where carbonate precipitation occurs is observed. The precipitation of minerals on cell envelopes generally results in a very fine precipitate (24). In this study, for *Scytonema* sp. strain ING-1 we can propose a mechanism similar to the one proposed for a cyanobacterial *Synechococcus* sp. (10, 26) and include the following biological and chemical reactions:

$$HCO_3^- + H_2O \rightarrow (CH_2O) + OH^- + O_2 \text{ (photosynthesis)} \quad (1)$$

$$HCO_3^- + OH^- \rightarrow CO_3^{2-} + H_2O \quad (2)$$

$$2CO_3^{2-} + 5Zn^{2+} + 6H_2O \rightarrow Zn_5(CO_3)_2(OH)_6 + 6H^+ \quad (3)$$

In spite of the acidity produced by reaction 3, the pH actually increases, being abundantly counterbalanced by the high photosynthetic activity.

Acidic polysaccharide (Alcian blue positive) binds Zn^{2+} and other metals. This metal binding, concomitant with CO_3^{2-} formation during photosynthesis, causes a local oversaturation with respect to the carbonate phase, thus favoring hydrozincite precipitation.

The formation of hydrozincite instead of the anhydrous-phase smithsonite reflects the chemical conditions imposed by biological activity. Both these secondary minerals are common in a mine environment. Hydrozincite is stable for log $pCO_2 > -5.2$, whereas smithsonite is stable at a higher level of pCO_2 (log $pCO_2 > -1.5$) (29).

The natural remediation of heavy metals produced by this photosynthetic population can probably be exported to other similar environments to attenuate metal pollution.

This research work was supported by MURST and CNR grants.
We thank L. Fanfani and P. Lattanzi for their criticism of the paper.

REFERENCES

1. **Baldi, F., V. P. Kukhar, and Z. R. Ulberg.** 1997. Bioconversion and removal of metals and radionuclides, p. 75–91. *In* J. R. Wild (ed.), Perspectives in bioremediation. Kluver Academic Publishers, Amsterdam, The Netherlands.
2. **Baldi, F., A. Minacci, A. Saliot, L. Mejanelle, O. Mozetic, V. Turk, and A. Malej.** 1997. Cell lysis and release of particulate polysaccharides in extensive marine mucillage assessed by lipid biomarkers and molecular probes. Mar. Ecol. Prog. Ser. **153:**45–57.
3. **Buurman, P., B. van Lagen, and E. J. Velthorst.** 1996. Total or organic carbon and total nitrogen (elemental analyzer), p. 11–16. *In* P. Buurman, B. van Lagen, and E. J. Velthorst (ed.), Manual for soil and water analysis. Backhuys Publishers, Leiden, The Netherlands.
4. **Caboi, R., R. Cidu, A. Cristini, L. Fanfani, R. Massoli-Novelli, and P. Zuddas.** 1993. The abandoned Pb-Zn mine of Ingurtosu, Sardinia (Italy). Eng. Geol. **34:**211–218.
5. **Caboi, R., R. Cidu, L. Fanfani, and P. Zuddas.** 1996. Abandoned mine sites: implications for water quality, p. 797–805. *In* R. Ciccu (ed.), Proceedings of the Fourth International Conference on Environmental Issues and Waste Management in Energy and Mineral Production, vol. 2. Department of Geoengineering and Environmental Technologies, University of Cagliari, Cagliari, Italy.
6. **Caboi, R., R. Cidu, L. Fanfani, P. Lattanzi, and P. Zuddas.** 1999. Environmental mineralogy and geochemistry of the abandoned Pb-Zn Montevecchio-Ingurtosu mining district, Sardinia, Italy. Chron. Rech. Minière **534:**21–28.
7. **Castenholz, R. W., and J. B. Waterbury.** 1989. Oxygenic photosynthetic bacteria, p. 1710–1806. *In* M. P. Bryant (ed.), Bergey's manual of systematic bacteriology, vol. 3. Williams & Wilkins, Baltimore, Md.
8. **Cidu, R.** (1996). Inductively coupled plasma - mass spectrometry and - optical emission spectrometry determination of trace elements in water. At. Spectrosc. **17:**155–162.
9. **Collins, Y. E., and G. Stotzky.** 1989. Factors affecting the toxicity of heavy metals to microbes, p. 31–90. *In* T. J. Beveridge and R. J. Doyle (ed.), Metal ions and bacteria. Wiley Interscience, New York, N.Y.
10. **Ehrlich, H. L.** 1998. Geomicrobiology: its significance for geology. Earth Sci. Rev. **45:**45–60.
11. **Ferris, F. G., R. G. Wiese, and W. S. Fyfe.** 1994. Precipitation of carbonate minerals by microorganisms: implications for silicate weathering and the global carbon dioxide budget. Geomicrobiol. J. **12:**1–13.
12. **Ferris, F. G., C. M. Fratton, J. P. Gerits, S. Schultze-Lam, and B. Sherwood-Lollar.** 1995. Microbial precipitation of a strontium calcite phase at a groundwater discharge zone near Rock Creek, British Columbia, Canada. Geomicrobiol. J. **13:**57–67.
13. **Fortin, D., F. G. Ferris, and T. J. Beveridge.** 1997. Surface-mediated mineral development by bacteria, p. 161–177. *In* J. F. Banfield and K. H. Nealson (ed.), Geomicrobiology: interactions between microbes and minerals. Reviews in mineralogy, vol. 35. Mineralogical Society of America, Washington, D.C.
14. **Fresenius, W., K. E. Quentin, and W. Schneider.** 1988. Water analysis. Springer-Verlag, Berlin, Germany.
15. **Gadd, G. M., and C. White.** 1993. Microbial treatment of metal pollution—a working biotechnology? Trends Biotechnol. **11:**353–359.
16. **Hunt, D. T. E., and A. L. Wilson.** 1986. Analytical techniques, p. 367–616. *In* D. T. E. Hunt and A. L. Wilson (ed.), The chemical analysis of water, 2nd ed. Royal Society of Chemistry, London, United Kingdom.
17. **Jambor, J. L.** 1964. Studies of basic copper and zinc carbonates. 1. Synthetic zinc carbonates and their relationship to hydrozincite. Can. Mineral. **8:**92–108.
18. **Kalin, M.** 1998. Biological polishing of zinc in a mine waste management area, p. 321–334. *In* W. Geller, H. Klapper, and W. Salomons (ed.), Acidic mining lakes: mine drainage, limnology, and reclamation. Springer-Verlag, Berlin, Germany.
19. **Luck, D., G. Piperno, Z. Ramanis, and B. Huang.** 1977. Flagellar mutants of *Chlamydomonas*: studies of radial spot-defective strains by dikarion and revertant analysis. Proc. Natl. Acad. Sci. USA **74:**3456–3460.
20. **Murray, R. G. E., R. N. Doetsch, and C. F. Robinow.** 1994. Determinative and cytological light microscopy, p. 21–41. *In* P. Gherhards, R. G. E. Murray, W. A. Wood, and N. R. Krieg (ed.), Methods for general and molecular bacteriology. American Society for Microbiology, Washington, D.C.
21. **Pala, A., L. G. Costamagna, and A. Muscas.** 1996. Valutazione delle riserve idriche nei bacini dei Rii Piscinas e Naracauli (Sardegna Meridionale). Boll. Soc. Geol. Ital. **115:**717–735.
22. **Salvadori, I., and P. Zuffardi.** 1973. Contributo alla conoscenza del giacimento piombo-zincifero di Montevecchio (Sardegna). Rend. Soc. Min. Ital. **20:**279–282.

23. **Sawicki, J. A., D. A. Brown, and T. J. Beveridge.** 1995. Microbial precipitation of siderite and protoferrihydrite in a biofilm. Can. Mineral. **33:**1–6.
24. **Stumm, W.** 1992. Chemistry of the solid-water interface. Wiley & Sons, New York, N.Y.
25. **Stumm, W., and J. J. Morgan.** 1981. Aquatic chemistry. Wiley & Sons, New York, N.Y.
26. **Thompson, J. B., and F. G. Ferris.** 1990. Cyanobacterial precipitation of gypsum, calcite, and magnesite from natural alkaline lake water. Geology **18:**995–998.
27. **Urrutia, M. M., and T. J. Beveridge.** 1994. Formation of fine-grained metal and silicate precipitates on a bacterial surface (*Bacillus subtilis*). Chem. Geol. **116:**261–280.
28. **Walkley, A., and I. A. Black.** 1934. An examination of the Degtjareff method for determining soil organic matter, and a proposed modification of the chromic acid titration method. Soil Sci. **34:**29–38.
29. **Williams, P. A.** 1990. Carbonate minerals, p. 174–196. *In* P. A. Williams (ed.), Oxide zone geochemistry. Ellis Horwood Ltd., New York, N.Y.
30. **Zuddas, P., F. Podda, and A. Lay.** 1998. Flocculation of metal-rich colloids in a stream affected by mine drainage, p. 1009–1012. *In* G. B. Arehart and J. R. Hulston (ed.), Proceedings of the 9th International Symposium on Water-Rock Interaction. Balkema, Rotterdam, The Netherlands.